Complete correlation studies of two-proton decays: ^{6}Be and ^{45}Fe

L.V. Grigorenko [a,b,c,∗], T.D. Wiser [d], K. Miernik [e], R.J. Charity [f], M. Pfützner [e], A. Banu [g], C.R. Bingham [h], M. Ćwiok [e], I.G. Darby [h], W. Dominik [e], J.M. Elson [f], T. Ginter [i], R. Grzywacz [h], Z. Janas [e], M. Karny [e], A. Korgul [e], S.N. Liddick [h], K. Mercurio [d], M. Rajabali [h], K. Rykaczewski [j], R. Shane [f], L.G. Sobotka [f,d], A. Stolz [i], L. Trache [g], R.E. Tribble [g], A.H. Wuosmaa [k], M.V. Zhukov [l]

[a] *Flerov Laboratory of Nuclear Reactions, JINR, RU-141980 Dubna, Russia*
[b] *Gesellschaft für Schwerionenforschung mbH, Planckstrasse 1, D-64291 Darmstadt, Germany*
[c] *Russian Research Center "The Kurchatov Institute", Kurchatov sq. 1, RU-123182 Moscow, Russia*
[d] *Departments of Physics, Washington University, St. Louis, MO 63130, USA*
[e] *Physics Department, University of Warsaw, 00-681 Warsaw, Poland*
[f] *Departments of Chemistry, Washington University, St. Louis, MO 63130, USA*
[g] *Cyclotron Institute, Texas A&M University, College Station, TX 77843, USA*
[h] *Department of Physics and Astronomy, University of Tennessee, Knoxville, TN 37996, USA*
[i] *National Superconducting Cyclotron Laboratory, Michigan State University, East Lansing, MI 48824, USA*
[j] *Physics Division, Oak Ridge National Laboratory, Oak Ridge, TN 37831, USA*
[k] *Department of Physics, Western Michigan University, Kalamazoo, MI 49008, USA*
[l] *Fundamental Physics, Chalmers University of Technology, S-41296 Göteborg, Sweden*

ARTICLE INFO

ABSTRACT

The complete three-body correlation pictures are experimentally reconstructed for the two-proton decays of the ^{6}Be and ^{45}Fe ground states. We are able to see qualitative similarities and differences between these decays. They demonstrate very good agreement with the predictions of a theoretical three-body cluster model. Validity of the theoretical methods for treatment of the three-body Coulombic decays of this class is thus established by the broad range of lifetimes and nuclear masses spanned by these cases. Implementations for decay dynamics and nuclear structure of $2p$ emitters are discussed.

© 2009 Elsevier B.V. All rights reserved.

1. Introduction

So-called "true" two-proton (true three-body) decays take place in the dripline nuclei where one-proton emission is energetically prohibited. In these situations the decay products should be emitted simultaneously, which cause distinct energy systematics and specific correlation patterns of such decays. From the theoretical side, two-proton radioactivity is part of a general quantum-mechanical three-body Coulomb continuum problem which appears in a number of different fields of physics.

Since the prediction of two-proton radioactivity, by Goldansky in 1960 [1], it was clear that $2p$ decays can provide important information about the structure of the parent system. However, for a long time it was not clear how this information could be extracted. Does information about the internal structure survive in the decay or is it completely lost in the process of the two protons penetrating the Coulomb barrier? The first notions about $2p$ decay were the "diproton" picture [1,2] which is still popular (e.g. [3,4]). Here the two protons are travelling under the barrier in the $S = 0$ state and can be considered as a single "diproton" particle. This is a quasiclassical (QC) approach as it assumes that the "rigid" diproton propagates under the barrier along a classical trajectory. In this picture most of the information about the nuclear interior is lost and we can only obtain information about the peculiarities of the final-state interaction from studying proton correla-

tions. Totally different predictions were provided by the quantum-mechanical theory of $2p$ radioactivity and three-body decay developed in Refs. [5,6]. This is a three-body cluster approach utilizing the hyperspherical-harmonics method with approximate boundary conditions for the three-body Coulomb problem. Exploratory studies of correlations performed in [7–9] predicted complex correlation patterns which are sensitive (in s/d shell nuclei) and very sensitive (in p/f shell nuclei) to the structure of the $2p$ emitter.

The $2p$ radioactivity is the latest found type of radioactive decay (experimentally discovered in ^{45}Fe in 2002 [10,11]) and the recent progress of this field is very fast. The new cases of $2p$ radioactivity were found in ^{54}Zn [12], ^{19}Mg [13], and further detailed studies of ^{45}Fe were performed in works [14–16]. Confirmation of the predictions of Refs. [8,9] were obtained in the papers [16,17] for inclusive correlation spectra of ^{45}Fe and ^{19}Mg decays. However, it is clear that the integrated distributions can only give a limited representation of the complete correlation picture. In this work, we provide, for the first time, a view of the $2p$ correlations in their "full glory" for the two important cases of ^{6}Be and ^{45}Fe. The ^{6}Be nucleus is the lightest true two-proton emitter in the sense offered by Goldansky and is an isobaric partner of the famous Borromean halo nucleus ^{6}He. Understanding the ^{6}Be system is important as it is the simplest case, and would thus provide a reliable basis for all further studies of two-proton decay. However, theoretical studies of ^{6}Be were limited, so far, mainly to the studies of energies and widths of the states (the complete correlations have never been calculated). The precise experimental data on correlations were also not existing. The last experimental work dedicated to correlations in ^{6}Be is almost 20 years old [18]. The ^{45}Fe nucleus is the first discovered case of $2p$ radioactivity [10,11] and the best studied so far [19]. Other heavy two-proton emitters should be best understood by this example.

2. ^{6}Be experiment

^{6}Be fragments were produced from the α-decay of ^{10}C projectiles excited via inelastic-scattering interactions on Be and C targets. An initial ^{10}B primary beam was delivered by the Texas A&M University K500 cyclotron facility and it impinged on a hydrogen gas cell. A secondary 10.7 MeV/A ^{10}C beam produced in the ^{10}B$(p,n)^{10}$C reaction was separated from other reaction products with the MARS spectrometer. The decay products (two protons and alpha) were detected in an array of 4 E–ΔE position-sensitive telescopes located downstream from the target. The complete kinematics was reconstructed for the ^{6}Be events and they were separated from the other decay channels. More details of the experiment and theory can be found in Refs. [20,21].

3. ^{45}Fe experiment

Ions of ^{45}Fe were produced at the National Superconducting Cyclotron Laboratory at Michigan State University, in the reaction of a ^{58}Ni beam at 161 MeV/A, with average intensity of 15 pnA, impinging on a 800 mg/cm^2 thick natural nickel target. The ^{45}Fe fragments were separated using the A1900 fragment separator and identified in flight by using time-of-flight vs. ΔE information. The $2p$ decay has been studied by means of a novel type of a gaseous detector employing digital imaging to record tracks of charged particles. Since publication [16] the data treatment has been improved, including the reconstruction of complete kinematics for ^{45}Fe events. Some details of the experiment are given in Ref. [16], the full description will be given in Ref. [22].

4. Two-proton correlations

In theoretical approach of Refs. [5,6] the three-cluster Schrödinger equation

$$(\hat{H}_3 - E_T + i\Gamma/2)\Psi^{(+)} = 0 \tag{1}$$

is solved using the hyperspherical harmonics method with the approximate boundary conditions of the three-body Coulomb problem formulated in Ref. [6]. The three-body decay energy E_T is fitted to experimental value using phenomenological three-body short-range potential. The width Γ and the WF $\Psi^{(+)}$ with pure outgoing asymptotic are found from Eq. (1). The momentum distributions of the decay products are obtained as differential flux through the hypersphere of the large hyperradius $\rho_{\max}$:

$$\frac{dj}{d\Omega_{3b}} = \frac{1}{M} \mathrm{Im}\left[\Psi^{(+)\dagger}\rho^{5/2}\frac{d}{d\rho}\rho^{5/2}\Psi^{(+)}\right]\Bigg|_{\rho_{\max}}, \tag{2}$$

where Ω_{3b} is a complete set of the three-body kinematical variables complementary to the energy E_T. If we forget about spins, there are nine degrees of freedom for decays with three particles in the final state. Three of them describe the center-of-mass (c.m.) motion, three describe the Euler rotation of the decay plane, and the three-body decay energy E_T is fixed. We end up with two parameters representing the complete correlation picture. It is convenient to choose an energy distribution parameter ε and an angle θ_k between the Jacobi momenta:

$$\varepsilon = E_x/E_T, \qquad \cos(\theta_k) = (\mathbf{k}_x \cdot \mathbf{k}_y)/(k_x k_y),$$

$$E_T = E_x + E_y = \frac{(A_1 + A_2)k_x^2}{2MA_1 A_2} + \frac{(A_1 + A_2 + A_3)k_y^2}{2M(A_1 + A_2)A_3},$$

$$\mathbf{k}_x = \frac{A_2\mathbf{k}_1 - A_1\mathbf{k}_2}{A_1 + A_2}, \qquad \mathbf{k}_y = \frac{A_3(\mathbf{k}_1 + \mathbf{k}_2) - (A_1 + A_2)\mathbf{k}_3}{A_1 + A_2 + A_3},$$

where M is nucleon mass and A_i are mass numbers of the particles. For two-proton emitters (protons are indistinguishable) there are two "irreducible" Jacobi systems, called "T" and "Y" (see top of Fig. 1). In the "T" Jacobi system, the core is the particle A_3 and parameter ε describes the energy distribution between the two protons. In the "Y" Jacobi system, the core is the particle A_2 and ε corresponds to core and proton subsystem. The Jacobi momentum $\mathbf{k}_x$ is the momentum of particle 1 in the c.m. of particles 1 and 2, $\mathbf{k}_y$ is the c.m. momentum of particles 1 and 2 in the c.m. of the whole system (particles 1, 2, and 3). Distributions constructed in the different Jacobi systems are just different representations of the same physical picture. Each Jacobi system can reveal different aspects of the correlation picture.

Complete correlation pictures for the ^{6}Be and ^{45}Fe g.s. decays are provided in Figs. 1 and 2. Schematic figures are included in Fig. 1 to help in visualizing the correlations associated with different regions of the Jacobi plots. Differences and similarities between the heavy and light $2p$ emitters can easily be seen in these plots.

The general features of the experimental correlations are reproduced by the theory. This can be confidently stated even for the relatively low ^{45}Fe statistics. Calculations shown in Figs. 1 and 2 were made in certain assumptions about internal structure of the decaying nuclei. We return to the relations between structure and lifetime for $2p$ emitters in Section 10, but before we would like to emphasize several important issues.

5. Timescales

The difference in the lifetimes $T_{1/2}$ of ^{6}Be and ^{45}Fe is striking: $5.0(3) \times 10^{-21}$ and $3.7(4) \times 10^{-3}$ s, respectively. This takes place because the $2p$ decay process probability has a very strong dependence on the decay characteristics, which can be roughly estimated as
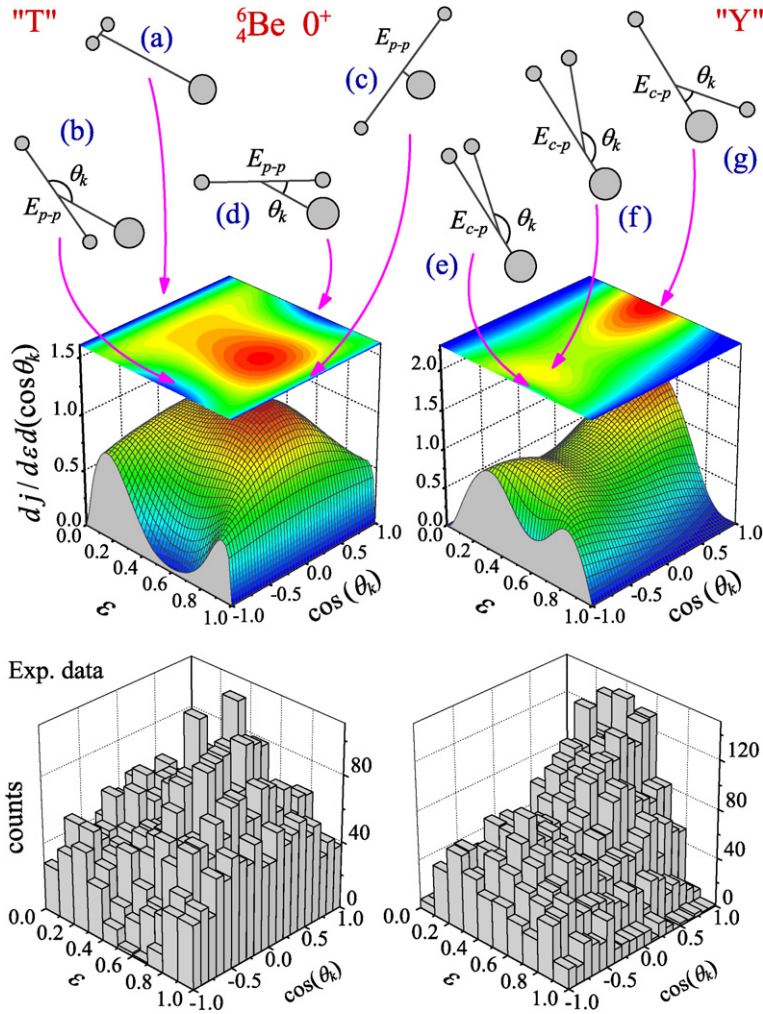
Fig. 1. (Colour online.) Complete correlation picture for ^{6}Be g.s. decay, presented in "T" and "Y" Jacobi systems (left and right columns, respectively). The upper row is theory, lower – experimental data.

$\Gamma \sim \exp[-4\pi Z_{\text{core}}\sqrt{2M/E_T}\,]$.

The coefficient in the exponent here is twice larger than for ordinary proton decays. The $2p$ decay theory manages the necessary range of lifetimes successfully.

6. Special kinematical regions

Despite the strong differences in Figs. 1 and 2 there are certain kinematical regions (illustrated on top of Fig. 1) where the decay dynamics is governed by the same physics.

Strong Coulomb suppressions due to the core–p repulsion occur in regions (b) and (d) and a smaller effect for the p–p channel is found in (e). The magnitude of the suppressions in (b) and (d) is significantly larger for the heavier ^{45}Fe case. On the other hand, the p–p final-state interaction gives rise to enhancements in regions (a) and (f). Although the g.s. core–p resonance is not energetically accessible for decay, the enhancement in region (g) is a hint of its presence.

It is clear that in the limits $\varepsilon \to 0$ and $\varepsilon \to 1$, the dependence on the relative orientation of $\mathbf{k}_x$ and $\mathbf{k}_y$ in the "T" system should become degenerate. The angular dependence practically vanishes for situations (a) and (c) but it can be seen in the theoretical plots that the scale of the phenomenon is very different: $\varepsilon \lesssim 0.2$ and $\varepsilon \gtrsim 0.9$ in ^{6}Be and $\varepsilon \lesssim 0.02$ and $\varepsilon \gtrsim 0.98$ in ^{45}Fe. In ^{6}Be this effect is seen, in ^{45}Fe these regions are not experimentally accessed

due to low statistics. At intermediate values of ε the angular dependence of distributions is very pronounced.

7. Any "diproton" decay?

In the framework of the "diproton" model, the differential decay probability in the "T" system can be estimated as

$$\frac{dj}{d\varepsilon} = 2\gamma_{pp}^2 \rho(\varepsilon E_T) P_0\big(E_T(1-\varepsilon), r_{\text{ch(dp)}}, 2Z_{\text{core}}\big). \tag{3}$$

The function P_l is a standard penetrability factor depending on the energy, channel radius, and charges, and $\rho(\varepsilon E_T)$ is the "density of diproton states". This density has been approximated as either a "fixed-energy diproton", i.e., $\rho(E) = \delta(E - E_0)$ with $E_0 \approx 50$ keV or alternatively for a "Coulomb-corrected phase volume", $\rho(E) = P_0(E, r_{\text{ch(pp)}}, 1)$. Finally, a treatment of this density in the spirit of the Migdal–Watson approximation can be found in Ref. [3].

Whatever approximation is chosen for density of the diproton states, the diproton model (3) should provide, in the "T" system, an angle-independent decay probability. However, the angular dependence in the "T" system is present in the experimental data (Figs. 1 and 2). Moreover, one can see that these angular distributions depend on energy between two protons (parameter ε). Thus the experimental data in the "T" system demonstrate that the $2p$ decay process cannot be approximated as diproton decay neither in the light (^{6}Be) nor in the heavy (^{45}Fe) systems.
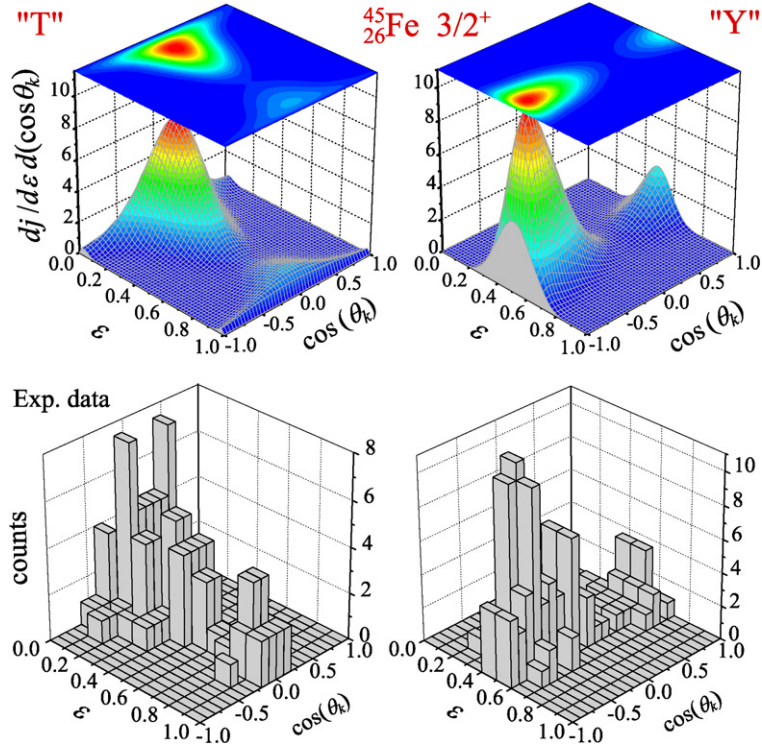
Fig. 2. (Colour online.) Complete correlation picture for ^{45}Fe g.s. decay, presented in "T" and "Y" Jacobi systems. The upper row is theory, lower – experimental data. Theoretical predictions are shown for the case of configuration mixing with $W(p^2) = 24\%$.

8. Common features of the energy distributions in "Y" system

The energy distribution in the "Y" system (see Figs. 3 and 4) is approximately a symmetric bell shape. This is the energy distribution between the core and one of the protons; its symmetry reflects the symmetry between protons. In heavy two-proton emitters, this distribution becomes very narrow and is almost completely symmetric. The shape of this distribution can be approximated by the quasiclassical expression [23,24]:

$$\frac{dj}{d\varepsilon} = \frac{E_T \langle V_3 \rangle^2}{2\pi} \frac{\Gamma_{p_1}(\varepsilon E_T)}{(\varepsilon E_T - E_{p1})^2 + \Gamma_{p_1}^2(\varepsilon E_T)/4}$$

$$\times \frac{\Gamma_{p_2}((1-\varepsilon)E_T)}{((1-\varepsilon)E_T - E_{p2})^2 + \Gamma_{p_2}^2((1-\varepsilon)E_T)/4},$$

$$\Gamma_{p_i}(E_i) = 2\gamma_i^2 P_{l_i}(E_i, r_{\text{chi}}, Z_i),$$

$$\langle V_3 \rangle^2 = D_3(E_T - E_{p1} - E_{p2})^2, \tag{4}$$

where E_{p_i} and Γ_{p_i} are parameters of the ground-state resonance in the core $+ p$ subsystem and the values of parameter $D_3 \sim 1$ MeV are realistic. For derivation of Eq. (4) two following assumptions about the subsystems could be reasonable (see Ref. [24] for details). (i) We can neglect the Coulomb interaction between protons. Then the "charges" for both subsystems should be taken $Z_i = Z_{\text{core}}$. This is the "no p–p interaction" case in Fig. 3; its profile does not reproduce the visible shift of experimental profile to the left. (ii) We can consider one of the subsystems as an effective particle with charge $Z_2 = Z_{\text{core}} + 1$ (while $Z_1 = Z_{\text{core}}$). In this "effective Coulomb" case the shift of the profile to the left is reproduced correctly, but the wings of the distribution are still wrong. The three-body calculations are in a near perfect agreement with the experimental data as shown in Fig. 3.
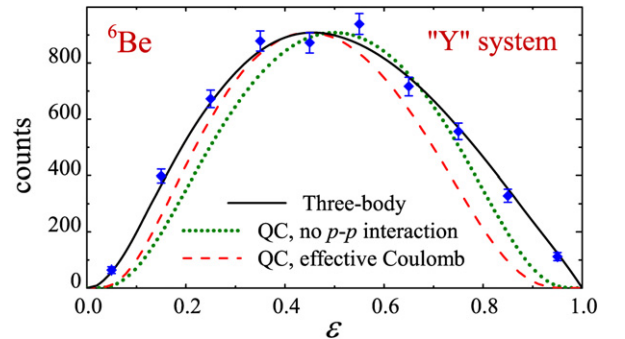

Fig. 3. (Colour online.) Energy distribution in "Y" system for ^{6}Be. Experimental data are shown by the diamonds with error bars.

9. Need for classical extrapolation in heavy $2p$ emitters

Certain aspects of the correlations are especially sensitive to the long-range nature of the Coulomb interaction. For example, the energy distribution in the "Y" system shown in Fig. 4 for ^{45}Fe is better reproduced with the quasiclassical approximation of Eq. (4) than with the calculations of Ref. [9]. The role of these long-range interactions was realized in [9], but not studied significantly. A classical extrapolation was suggested as an opportunity to deal with this problem: the quantum-mechanical model propagates the wave function (WF) to large distances (it was 1000 fm in [9]). Vectors of flux calculated at this radius are used as initial conditions for classical trajectories which are propagated until complete stability of the momentum distributions is obtained. For ^{45}Fe the distances around 50000 fm are found to be sufficient. It can be seen in Fig. 4 that the theoretical distributions after the classical extrapolation (dotted curve) are in nice agreement with the data. Classical extrapolation is also important for the angular distribution in the "T" system allowing one again to obtain excel-
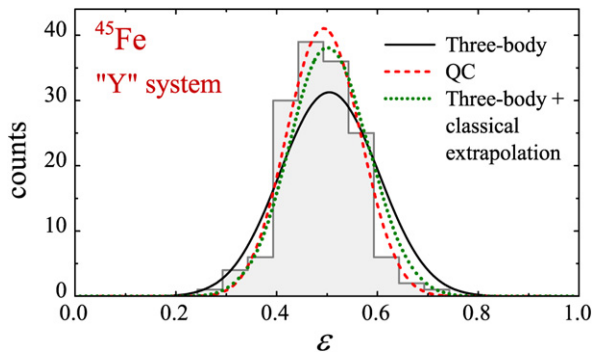
Fig. 4. (Colour online.) Energy distribution in "Y" system for ^{45}Fe. Experimental data are shown by the gray histogram.
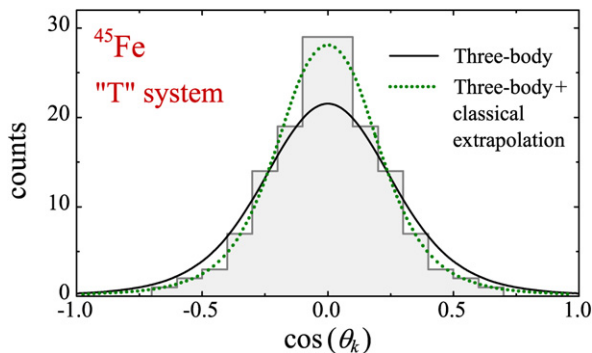

Fig. 5. (Colour online.) Angular distribution in "T" system for ^{45}Fe. Experimental data are shown by the gray histogram.

Fig. 6. (Colour online.) Energy distribution in "T" system for ^{6}Be. The grey and black curves show the theoretical distributions before and after the detector bias was included via a Monte Carlo (MC) simulation. Experimental data are shown by the diamonds with error bars.

Fig. 7. (Colour online.) Energy distribution in "T" system for ^{45}Fe. Experimental data are shown by the gray histogram.

lent agreement with the data (see Fig. 5). However, other inclusive distributions (like those shown in Figs. 6 and 7) are practically insensitive to this aspect of the dynamics.

10. Details of structure

The energy distributions in "T" system has a double-humped profile both for ^{6}Be and ^{45}Fe which is an indication of the important contribution of the $[p^2]$ configuration. Note that this double-humped profile is expressed more in coordinate space [25].

The sensitivity of the correlations to the nuclear structure is illustrated in Figs. 6 and 7. Predictions for two core–p potentials in the ^{6}Be system are shown in Fig. 6. The Sack–Biedenharn–Breit (SBB, Ref. [26]) potential is used in the calculations with Gaussian parameterized formfactors where original radius value is $r_0 = 2.30$ fm. This provides $\Gamma = 112$ keV in a good agreement with experimental value [92(6) keV]. The α–n potential with increased (compared to the values deduced from the α–n scattering) size or depth was used in a number of calculations to improve binding energy. For example, in [5,25] the SBB potential with increased radius $r_0 = 2.35$ fm was used. This produced only a small effect on the phase shifts and was considered a reasonable improvement. The calculations with this modified SBB potential produced an unacceptable width of $\Gamma = 154$ keV. The predicted energy distributions are also noticeably different in Fig. 6. Comparison of theory and experiment for the full correlations of Fig. 1 gives $\chi^2/\nu = 1.17$ and 1.58 for $r_0 = 2.30$ and 2.35 fm, respectively. Thus the $2p$ correlations have a large sensitivity to the different aspects of the dynamics.

A strong dependence of the momentum distributions on the p^2/f^2 configuration mixing $W(p^2)$ was predicted for ^{45}Fe in Ref. [9]. This was confirmed in Ref. [16] for the angular distribution between the two protons. Similar strong sensitivity can be
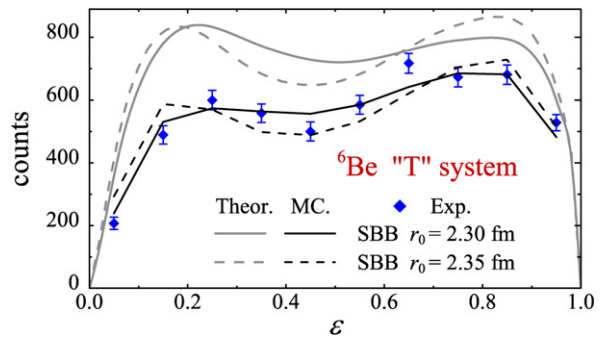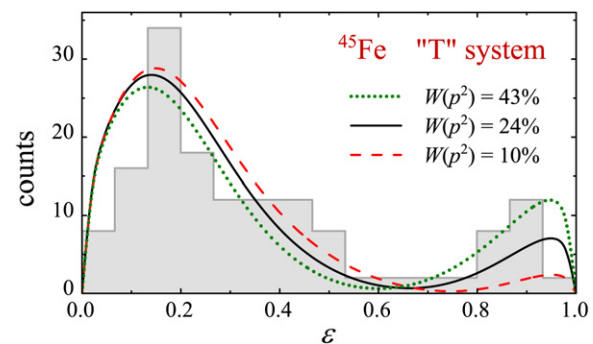
seen in Fig. 7 for the energy distribution between the two protons. The theoretical curves with $W(p^2)$ equal to 10, 24, and 43% have χ^2/ν equal to 18.7, 4.3, and 3.1, respectively. With a parabolic interpolation, the χ^2/ν is minimized with a configuration mixing ratio of 31%. It is important to notice that the lifetime of ^{45}Fe was predicted in Ref. [9] to be in the range ~ 700 μs–20 ms, for configuration mixing $W(p^2)/W(f^2)$ varying from 1 to 0. Within the achieved experimental precision (the ^{45}Fe $2p$ lifetime is 3.7(4) ms [16] and the decay energy is $E_T = 1.154(16)$ MeV [14]) the theoretically predicted lifetimes, allow for configuration mixing in the range $18 < W(p^2) < 45\%$. This range is consistent with the $W(p^2) = 31\%$ inferred above from the energy distribution.

11. Conclusion

The complete correlation pictures of $2p$ decays for ^{6}Be and ^{45}Fe are measured (and ^{6}Be also calculated) for the first time. These correlations have common features (e.g., connected with significant weight of $[p^2]$ component in the WF) as well as differences (e.g., connected with the larger Coulomb repulsion in heavy $2p$ emitter and admixture of $[f^2]$ configuration). High statistics data in ^{6}Be allows for a discussion of the fine details of correlation patterns. The ^{45}Fe data, despite the quite low statistics, indicate that certain improvements in the theoretical treatment of the process are necessary.

Features of the three-body correlations are well reproduced by the quantum-mechanical model in a broad range of times and masses: from typical nuclear times ($\sim 10^{-20}$ s in ^{6}Be) to typical radioactivity times (some milliseconds in ^{45}Fe). The quasiclassical expression can provide a reasonable approximation for certain distributions. However, it fails if we consider these distributions in fine details or if we look on the whole correlation picture. Certain aspects of correlations (e.g., ε distribution in the "T" system)

can be highly sensitive to the fine details of nuclear structure. This makes the complete correlation studies of $2p$ emitters a promising tool for the structure research.

Theoretical models are further constrained when consistent descriptions of the widths and correlations are made simultaneously. This provides a cross check of the extracted structure information which has never been accessible before.

Acknowledgements

References

[1] V.I. Goldansky, Nucl. Phys. 19 (1960) 482.
[2] V.I. Goldansky, Nucl. Phys. 27 (1961) 648.
[3] F.C. Barker, Phys. Rev. C 63 (2001) 047303.
[4] B.A. Brown, F.C. Barker, Phys. Rev. C 67 (2003) 041304(R).
[5] L.V. Grigorenko, R.C. Johnson, I.G. Mukha, I.J. Thompson, M.V. Zhukov, Phys. Rev. Lett. 85 (2000) 22.
[6] L.V. Grigorenko, R.C. Johnson, I.J. Thompson, M.V. Zhukov, Phys. Rev. C 65 (2002) 044612.
[7] L.V. Grigorenko, I.G. Mukha, I.J. Thompson, M.V. Zhukov, Phys. Rev. Lett. 88 (2002) 042502.
[8] L.V. Grigorenko, I.G. Mukha, M.V. Zhukov, Nucl. Phys. A 713 (2003) 372;
L.V. Grigorenko, I.G. Mukha, M.V. Zhukov, Nucl. Phys. A 740 (2004) 401, Erratum.
[9] L.V. Grigorenko, M.V. Zhukov, Phys. Rev. C 68 (2003) 054005.
[10] M. Pfützner, et al., Eur. Phys. J. A 14 (2002) 279.
[11] J. Giovinazzo, et al., Phys. Rev. Lett. 89 (2002) 102501.
[12] B. Blank, et al., Phys. Rev. Lett. 94 (2005) 232501.
[13] I. Mukha, et al., Phys. Rev. Lett. 99 (2007) 182501.
[14] C. Dossat, et al., Phys. Rev. C 72 (2005) 054315.
[15] J. Giovinazzo, et al., Phys. Rev. Lett. 99 (2007) 102501.
[16] K. Miernik, et al., Phys. Rev. Lett. 99 (2007) 192501.
[17] I. Mukha, et al., Phys. Rev. C 77 (2008) 061303(R).
[18] O.V. Bochkarev, et al., Nucl. Phys. A 505 (1989) 215.
[19] B. Blank, M. Ploszajczak, Rep. Prog. Phys. 71 (2008) 046301.
[20] K. Mercurio, et al., Phys. Rev. C 78 (2008) 031602(R).
[21] L.V. Grigorenko, et al., arXiv:0812.4065.
[22] K. Miernik, et al., Eur. Phys. J. A (2009), in press.
[23] V.M. Galitsky, V.F. Cheltsov, Nucl. Phys. 56 (1964) 86.
[24] L.V. Grigorenko, M.V. Zhukov, Phys. Rev. C 76 (2007) 014009.
[25] B.V. Danilin, et al., Phys. Rev. C 43 (1991) 2835.
[26] S. Sack, L.C. Biedenharn, G. Breit, Phys. Rev. 93 (1954) 321.